AN OVERVIEW OF A COOL SEASON

TORNADIC SUPERCELL OVER CENTRAL MISSISSIPPI

Alan E. Gerard[(1)]

Gregory R. Garrett

Clay Morgan

National Weather Service Forecast Office, Jackson, Mississippi

Abstract

Shortly after 0000 UTC on 10 December 1999, a relatively low topped supercell moved along the Big Black River in central Mississippi, producing a short track F3 tornado near the small town of Bentonia. This paper will present a multiscale meteorological analysis of the event. To begin, the overall synoptic pattern will be discussed, as well as the near storm environment as indicated by the 0000 UTC 10 December upper air sounding from Jackson, MS (JAN), which was a near proximity sounding for the storm. Storm scale analysis utilizing Weather Surveillance Radar-88 Doppler (WSR-88D) data will then be presented. Additionally, implications that this event has for the warning process will be discussed.

1. INTRODUCTION

Shortly after 0000 UTC on 10 December 1999, a relatively low topped (echo top less than 32 kft) supercell moved along the Big Black River in central Mississippi, producing a short track F3 tornado near the small town of Bentonia (Fig. 1). This supercell developed in advance of a pre-frontal squall line, and was the only known tornadic supercell in the region for this event.

This paper will begin by looking at this sounding, which was characterized by weak instability and relatively low values of storm-relative helicity, but strong deep-layer shear, as well as the synoptic environment. The role of the pre-storm environment in the evolution of this storm will be discussed. Then, a Weather Surveillance Radar-88 Doppler (WSR- 88D) radar discussion will be presented, including the evolution of several distinct reflectivity features which were observed. Additionally, the operational use of time series of velocity parameters in monitoring rotational trends and tornadogenesis mode during the lifetime of a storm will be discussed. The implications that this storm has for the warning process will also be presented.

2. PRE-STORM ENVIRONMENT

The synoptic pattern of 9-10 December 1999 was characterized by a deepening upper low moving through the central plains states, well to the northwest of Mississippi. However, to the east of this low, a well defined middle and upper tropospheric wind maximum was in place across the middle Mississippi valley. This wind maximum was in a favorable position during the evening hours such that northern and western Mississippi were in the right entrance region, with the jet induced ageostrophic circulation likely providing broad scale upward vertical motion over the region. This was in advance of a surface cold front which was approaching the region from the northwest. A line of strong thunderstorms was already in progress at 0000 UTC over extreme western Mississippi and northeastern Louisiana. This activity developed in an axis of Convective Available Potential Energy (CAPE) values near 1000 J kg^{-1} ahead of the cold front.

Ahead of the main convective line, scattered convection developed in a marginally unstable airmass. Most of this convection was ordinary multicell clusters; however, one storm did become supercellular, tracking through northern Warren and southern Yazoo counties (see Fig. 1), about 50 nmi northwest of the Jackson, MS (JAN) upper air site, shortly after 0000 UTC. Due to the temporal and spatial proximity of this storm to the JAN site, the 0000 UTC JAN upper air sounding was a near-proximity sounding for this storm.

This upper air sounding was analyzed (Fig. 2) using the N/AWIPS - Skew-T/Hodograph Analysis and Research Package (N-SHARP, Hart, et. al 1997). CAPE values were quite marginal for supercellular storms, with a value of 678 J kg^{-1}. The 0 to 3 km storm-relative environmental helicity (SREH) value, a parameter commonly used operationally to forecast the likelihood of tornadic storms (Davies-Jones and Burgess 1990), was 146 m^2s^{-2}, which is a value generally considered quite marginal for tornadic storms. The resulting combined Energy Helicity Index (EHI) was 0.76, which is below the commonly accepted value of 2.0 for tornadic storms, and well below the value of 3.0 which is operationally utilized as a cutoff for strong and violent tornadoes (Davies 1993).

Comparing the sounding parameters to a climatology developed by Rasmussen and Blanchard (1998) indicates that the CAPE, SREH, and EHI for this event were all well below the mean for tornadic storms. However, they were in the "window" of probability for tornadic storms above the 25th percentile. Additionally, the 0 to 2 km SREH was actually greater (176 m s^{-2}) than the 0 to 3 km value, indicative of the available SREH being concentrated near the ground which may mean the SREH was more favorable for tornadic storms than indicated by the 0 to 3 km SREH. Deep layer shear parameter values were quite large and indicative of the potential for supercellular storms. The Bulk Richardson Number shear value was 98 m^2s^{-2}, which is well above the operationally accepted value of 40 m^2s^{-2} required for supercellular storms. The combination of marginal instability and strong deep layer shear appears to have provided a somewhat favorable environment for supercellular storms ahead of the main squall line moving through extreme western Mississippi and northeastern Louisiana at 0000 UTC.

3. RADAR ANALYSIS OF SUPERCELL STORM

a. *Methodology*

The National Weather Service forecast office at Jackson (NWSFO JAN) utilizes the National Severe Storms Laboratory's (NSSL) Next Generation-Warning Decision Support System (NG-WDSS, see Gerard and Conway 2000) as its primary analysis tool for Weather Surveillance Radar-88 Doppler (WSR-88D) data during severe weather operations. The radar display software with NG-WDSS is the Radar Analysis and Display System (RADS), which can be utilized for post-storm analysis as part of the WSR-88D Algorithm Testing And Display System (WATADS, NSSL 1999).

The evolution of this storm was examined utilizing the WATADS software. As a part of RADS, derived and base reflectivity and velocity data can be viewed in planar and cross-section views. Additionally, output from NSSL algorithms such as the Mesocyclone Detection Algorithm (MDA, Stumpf, et.al 1998) and Tornado Detection Algorithm (TDA, Mitchell, et.al 1998) can be viewed, as well as time series of values generated by the algorithms. Discussions based on all of these different products from WATADS will be presented below, and it is important to note that these products were available and utilized by NWS personnel in Jackson for warning operations during this event.

Two unique parameters which can be displayed from the MDA using RADS are the Mesocyclone Strength Index (MSI) and the Strength Rank. These are non-dimensional values which indicate to the meteorologist the strength of the circulation as determined by the algorithm. In general, a circulation must be at least a rank 5 to be considered a mesocylone; the MSI value must reach 2300 to be considered a moderate mesocyclone and be greater than 3600 to be a strong mesocyclone (NSSL 1999).

b. *Overview of Storm Evolution*

The cell of interest developed on the Jefferson/Claiborne county line near the Mississippi River around 2245 UTC 9 December as part of a multicellular cluster of storms. Already at this time, a line of storms from southeast Arkansas to northeast Louisiana was approaching from the west. The multicellular cluster of storms was tracking northeast. From 2355 to 0011 UTC the northern two cells of this cluster began weakening while the southern cell intensified rapidly. The reflectivity core associated with the storm intensified with 55 dBZ values increasing in depth from 16 kft to 21kft. Storm-relative velocity products indicated an increase in mid level convergence and upper level divergence, while cross sections of reflectivity generated by WATADS indicated that a weak echo region was developing on the inflow side of the southern portion of the storm.

By 0011 UTC (Fig. 3), WATADS indicated a mesocyclone with a mesocyclone rank value of 5. The WATADS MDA indicated a 46 kt maximum gate-to-gate velocity difference; WATADS planar views of velocity and reflectivity indicated that this mainly mid level circulation was near the weak echo region and a developing inflow notch on the southern end of the storm. The reflectivity in the core of the storm had continued to increase and was now 63 dBZ extending to around 18 kft. At 0016 UTC, a slight decline in the circulation was indicated by the MDA with only a rank 4 weak circulation indicated with 52 kt maximum gate to gate velocity difference, a maximum shear of .017 s^{-1} and a mesocyclone depth of 10 kft. A low level reflectivity pendant was also becoming more visible as the mid level rotation was becoming more cyclonically convergent. The weak echo region had become more impressive with height and was now bounded above 6 kft.

Once again at 0021 UTC (Fig. 4) a rank 5 mesocyclone was indicated by the MDA with the MSI now 3827. By 0026 UTC, low level rotational velocity values showed an indication of an increase, now 40 kt at the 0.5 degree elevation angle with the maximum rotational velocity, 44 kt, at the next elevation or around 4 kft. Although the low level pendant was still visible, the reflectivity structure aloft was more indicative of a bow echo with a rear inflow notch noticeable on the southwest flank. This may have been an indication of a descending rear flank downdraft and a possible precursor of tornadogenesis.

At 0031 UTC (Fig. 5), the MDA and TDA indicated a TVS/Mesocyclone with the storm. The lowest elevation gate to gate velocity difference dramatically increased to 84 kt and was now also the maximum anywhere in the storm. Again in the reflectivity, an impressive rear inflow notch was observed aloft on the southwest flank of the storm. A well developed weak echo region continued to develop aloft over the low level inflow notch. An investigation of planar views of storm relative velocity revealed a strong rotational velocity couplet in the lowest two elevation angles, with much weaker rotation above this.

By 0036 UTC (Fig. 6), a TVS continued to be indicated by the TDA with the MDA yielding an MSI of 5581. Rotational velocity values continued to increase with low level and maximum gate to gate velocity difference now at 114 kt with a shear of .047 s^{-1}. Eight panel representations of reflectivity and storm relative velocity data produced by WATADS continued to yield evidence of a rear flank downdraft descending into the lower levels of the storm, while in the reflectivity, a marked collapse in the storm core was apparent. The first reports of a tornado were received at this time.

Little change in the low level velocity data was noted on the next volume scan at 0041 UTC. Rotational velocity values aloft were becoming even less impressive. The reflectivity structure also continued to show a drastic decrease in intensity and depth. A TVS continued to be indicated by the TDA at 0046 UTC, but rotational velocity values had decreased. While the maximum gate to gate was still at the lowest levels, values had decreased to 54 kt, and the overall rotational pattern had become much broader. There was some still some evidence of a slight weak echo region, but only in the very lowest levels as reflectivity continued to decrease. Based on surface reports, this volume scan is assumed to be the time of the dissipation of the tornadic vortex.

By 0051 UTC (Fig. 7), the MDA indicated a rank 5 low top mesocyclone with an MSI of 3839. While the rotational velocity values did increase slightly at 1.5 degrees (actually weakly divergent), the remaining elevations showed little in the way of rotation, and the rotation in the lower levels appeared to be primarily due to linear shear. The reflectivity data indicated that the original cell had occluded.

c. ***Time/Height Series***

With the availability of WDSS at NWSFO JAN, radar products other than the standard planar and cross-sectional views are available to the warning meteorologist. Meteorologists at NWSFO JAN have found that examination of time/height trend plots of reflectivity and velocity parameters output from the NSSL WDSS algorithms are an excellent means of monitoring trends within a given storm. As an example, time/height trend plots of velocity parameters from the MDA and TDA can assist in monitoring the rotational trends within a storm, and can assist in determining the tornadogenesis mode of a given storm as discussed by Trapp, et. al (1999).

A time series of rotational velocity is shown for the tornadic supercell discussed above is shown in Fig. 8. As can be seen, from 0016 UTC to 0036 UTC, the middle and upper level rotation associated with this supercell dramatically dissipated while rotation rapidly increased in the lower levels of the storm, particularly at and below 7 kft. The rotation at the 0.5 degree elevation angle increased from very little at 0011 UTC to 60 kt at 0036 UTC, which was the approximate tornadogenesis time.

Another time/height series which is often used operationally at NWSFO JAN is a plot of shear (Fig. 9). This plot clearly indicated a rapid increase in shear values between 0016 and 0036 UTC below 4 kft, peaking at .047 s^{-1} at 0036 UTC. It should be noted that in Figs. 7 and 8 that prior to 0016 UTC, the mesocyclone associated with the supercell was being identified by a different number by the MDA, and that deep, mainly mid level, rotation of 20 to 30 kt was present between about 2355 UTC and 0016 UTC as discussed in section 3b (see Fig. 10). After that time, however, the rotation above about 10 kft decreased dramatically while below that level rotation increased dramatically, peaking at the lowest two volume scans (an elevation of 1.5 kft to 4 kft) the volume scan prior to and the volume scan of tornadogenesis.

4. DISCUSSION AND WARNING IMPLICATIONS

WSR-88D observations indicate that the storm which produced the F3 tornado near Bentonia, MS at 0036 UTC 9 December initially developed as a part of a multicellular cluster of storms. Around 0000 UTC, the storm began to develop mid level rotation and reflectivity characteristics indicative of a supercell. Between 0000 UTC and 0016 UTC, the storm maintained weak to moderate mid level rotation. After this time, the circulation above 10 kft weakened dramatically in the 20 minutes leading up to tornadogenesis. By 0031 UTC there was little discernible rotation above 10 kft, and by 0041 UTC (5 min after the tornado touched down and while the tornado was still on the ground) there was little in the way of rotation above 7 kft. At the same time, rotational velocity increased very rapidly in the lower levels of the storm, peaking near the surface at tornadogenesis time.

In this case, radar products (not shown) did indicate that an area of weak convection moved across Yazoo county prior to the approach of the supercell, and between 0000 and 0011 did show the presence of a weak fine line just to the south of the area where the storm later passed through. While there is not sufficient evidence to say definitively that there was a defined boundary left by this initial weak convection which the supercell then interacted with, it seems probable that the storm interacted with a local source of horizontal vorticity which assisted tornadogenesis with this storm (as per Markowski, et. al 1998) and may have resulted in greater SREH values in the local area of the storm than observed on the 0000 UTC JAN sounding.

While the rotational velocity trends through the entire life of this particular storm do not seem to clearly fit either the non-descending or descending TVS mode as discussed by Trapp, et. al (1999), it is clear that during the critical four volume scans leading up to tornadogenesis, the rapid increase in rotational velocity took place mainly at or below 7 kft, while rotation above dramatically weakened. This rapid increase in low level rotation while mid level rotation was weakening made warning effectively for this storm a challenge. As will be discussed below, this challenge would have been much greater had the storm been farther away where radar horizon problems would have been a larger factor.

It should be pointed out that the means to operationally determine if the pre-storm environment favors a given mode of tornadogenesis could be of tremendous assistance to the warning meteorologist. In this event, the JAN 0000 UTC upper air sounding indicated that instability was weak and SREH was not particularly large. Hence, one could speculate that although supercells might develop, tornadogenesis would most likely occur when storms interacted with a local source of low level horizontal vorticity (e.g., a boundary per Markowski, et. al. 1998) or as part of bowing segments within the main squall line. Research by Trapp, et. al (1999) indicates that the latter type of tornadogenesis is more commonly associated with non-descending TVS signatures, and operational experience at NWSFO JAN suggests that the former process may be more frequently associated with non-descending TVS signatures as well. Further research should pursue more proven means of discriminating environments more favorable for a given TVS mode, enabling warning meteorologists to more easily anticipate tornadogenesis and issue the most effective warnings possible.

Even if the warning meteorologist is fully anticipating rapid intensification of low level rotation as is commonly observed in non-descending TVS development, it would remain very difficult to warn with a tremendous amount of lead time for these types of storms. In this event, the earlier presence of mid level rotation and development of reflectivity structures indicative of a supercell likely aided the warning process, and the proximity of the storm to the radar made monitoring low level trends of rotation possible. A tornado warning was issued by NWSFO JAN with about 10 min lead time. Reliance upon an algorithm identified TVS would have resulted in a lead time of virtually zero.

Warning meteorologists should always be cognizant of the potential for a storm to interact with a boundary, and when seeing such a potential interaction should be keenly aware of the possibility of rapid tornadogenesis with the storm involved. All means of boundary detection (radar, satellite, surface data, etc.) should be utilized to monitor such events. This may be a means of increasing lead times with such storms, although, as in this case, such boundary interactions can be subtle and difficult to discern.

Another challenge from this type of event was the low topped nature of the storm and the concentration of rotation in the lowest levels of the storm. The echo top of this storm never exceeded 32 kft, and Vertically Integrated Liquid values never exceeded 37 kg m^{-2}. Hence, reflectivity patterns and velocity data would have to be relied upon in the warning decision. Also, as can be seen in Fig. 8, the significant rotational velocity values during the tornadogenesis process were mainly confined to below 10 kft. Clearly, radar horizon problems would reduce the ability to discern significant rotation and effectively warn for this type of storm at greater ranges from the radar. If the storm had been beyond a range of about 75 nmi, velocity data from the lowest elevation angle would have likely indicated a decreasing trend in rotation during the tornadogenesis period, potentially hampering the issuance of effective warning products.

Finally, this case also demonstrates that large values of CAPE, 0 to 3 km SREH, or EHI are not required to have strong or violent tornadoes, as the near proximity sounding for this strong tornado had marginal values for these parameters. Parameters such as storm-relative winds or 0 to 1 km SREH, while not discussed here, may have proved more useful in indicating the tornadic potential for this event, and will be examined in future research.

5. REFERENCES

Davies, J.M., 1993: Hourly helicity, instability, and EHI in forecasting supercell tornadoes. *Preprints,* 17th Conference on Severe Local Storms, St. Louis, Amer. Met. Soc., 107-111.

Davies-Jones, R. and D. Burgess, 1990: Test of helicity as a tornado forecast parameter. *Preprints,* 16th Conference on Severe Local Storms, Kananaskis Park, AB, Canada, Amer. Met. Soc., 588-598.

Gerard, A.E. and J.W. Conway, 2000: Utilizing the NSSL Next Generation Warning Decision Support System in real-time warning operations at the Jackson, Mississippi National Weather Service. *Preprints*, 20th Conference on Severe Local Storms, Orlando, Amer. Met. Soc.

Hart, J.A., R. Lindsay and J. Whistler, 1997: N-SHARP: Advanced Interactive Sounding Analysis Program for NAWIPS.

Markowski, P.M., E.N. Rasmussen, J.M. Straka, 1998: The occurrence of tornadoes in supercells interacting with boundaries during VORTEX-95. *Wea. Forecasting,* **13,** 852-859.

Mitchell, E.D., S.V. Vasiloff, G.J. Stumpf, A. Witt, M.D. Eilts, J.T. Johnson, and K.W. Thomas, 1998: The National Severe Storms Laboratory Tornado Detection Algorithm. *Wea. Forecasting*, **13**, 352-366.

National Severe Storms Laboratory, 1999: WATADS: WSR-88D Algorithm Testing and Display System. Documentation available at http://www.nssl.noaa.gov/~watads/

Rasmussen, E.N. and D.O. Blanchard, 1998: A baseline climatology of sounding-derived supercell and tornado forecast parameters. *Wea. Forecasting*, **13**, 1148-1164.

Stumpf, G.J., A. Witt, E.D. Mitchell, P.L. Spencer, J.T. Johnson, M.D. Eilts, K.W. Thomas, and D.W. Burgess, 1998: The National Severe Storms Laboratory Mesocyclone Detection Algorithm for the WSR-88D. *Wea. Forecasting*, **13**, 304-326.

Trapp, R.J.; E.D. Mitchell; G.A. Tipton, D.W. Effertz, A.I. Watson, D.L. Andra, and M.A. Magsig, 1999: Descending and non-descending TVS signatures detected by WSR-88Ds. *Wea. Forecasting,* **14,** 625-639.

Fig. 1. Map indicating track of F3 tornado over Yazoo County, MS near the town of Bentonia. River just to the southeast of the track is the Big Black, northwest edge of the Jackson, MS metro area can be seen as the ground clutter return in the southeast corner of the image. Warren County lies just to the southwest of Yazoo County.

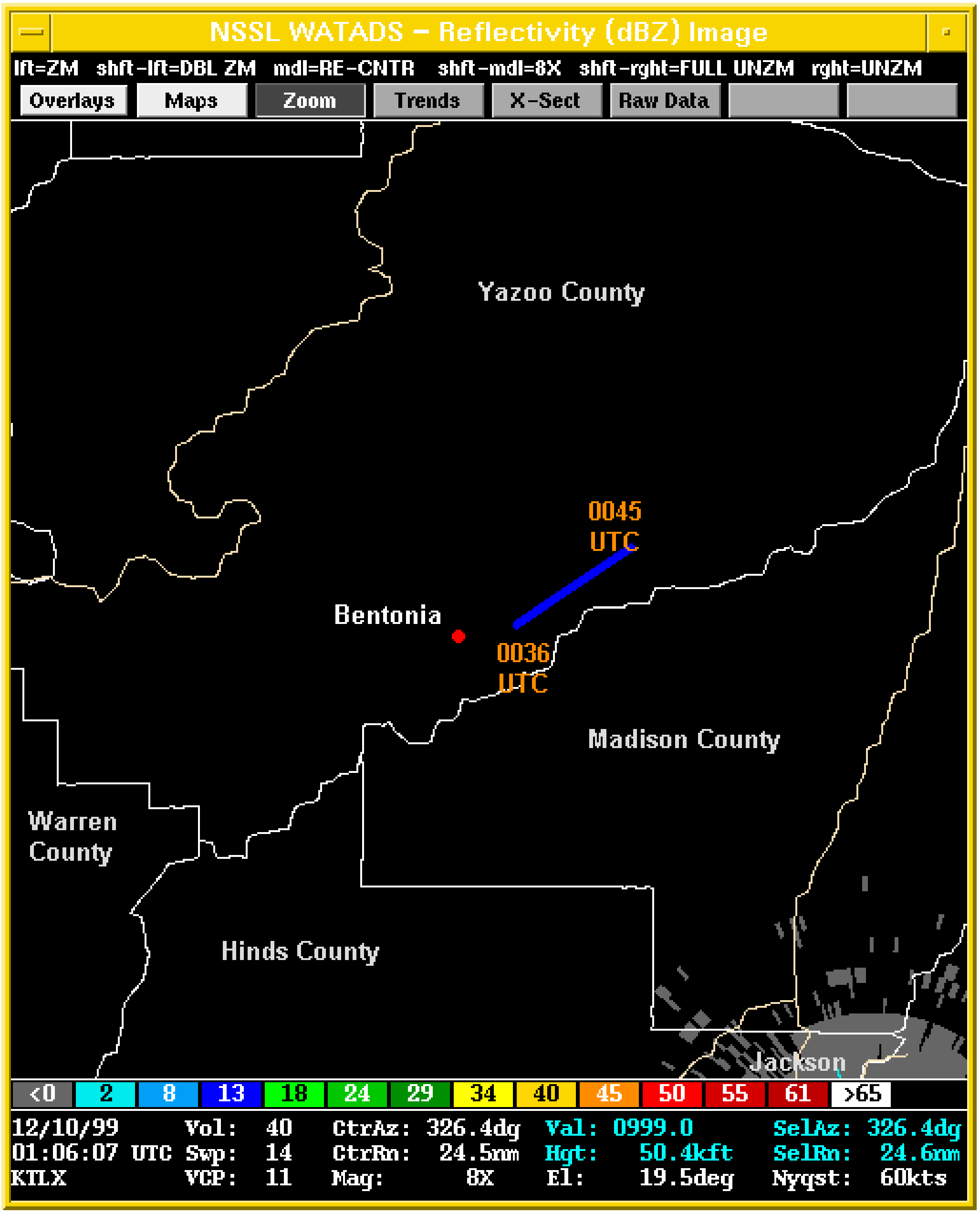

Fig. 2. Skew-T/log-P depiction of the 0000 UTC 10 December 1999 upper air sounding from Jackson, MS.

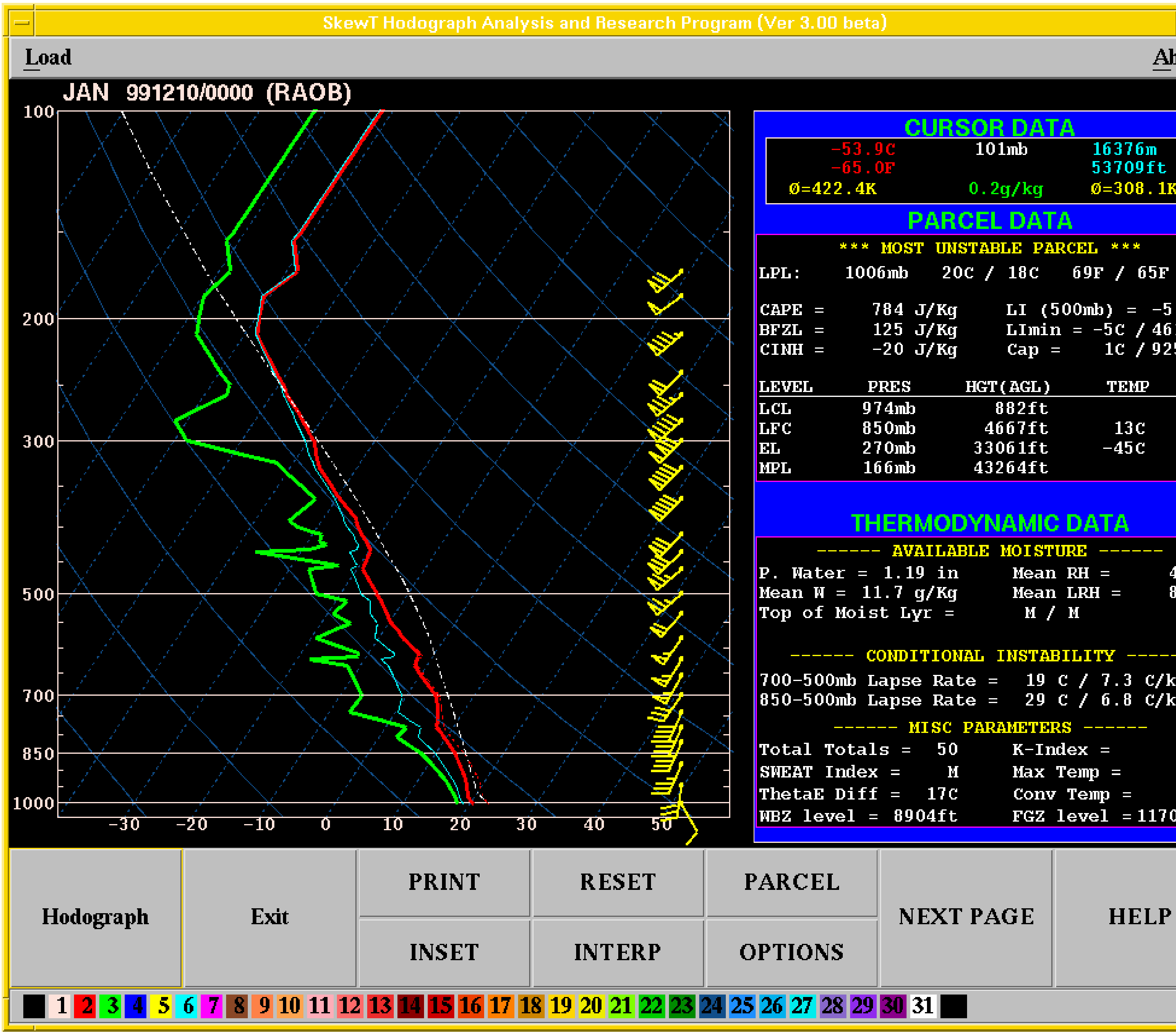

Fig. 3. 8 panel radar display from the Jackson, MS, WSR-88D radar valid at 0011 UTC 10 December 1999. Top images are reflectivity, bottom images are storm relative velocity. From left to right, elevation angles are 0.5 degrees, 1.5 degrees, 3.4 degrees, and 6.0 degrees. The storm of interest is storm number 46 in the cell algorithm table.

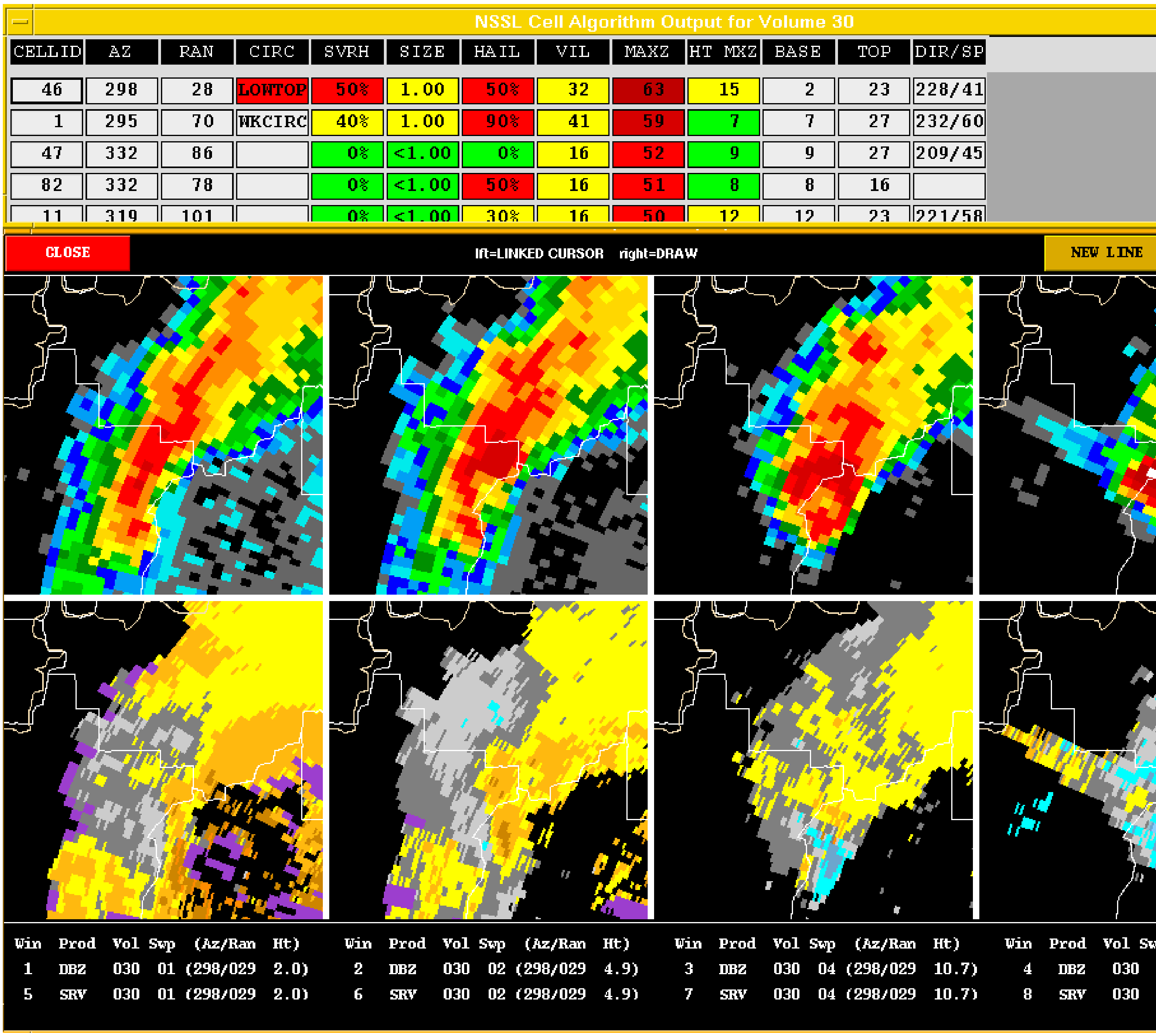

Fig. 4. Same as Fig. 3, only 0021 UTC.

NSSL Cell Algorithm Output for Volume 32

CELLID	AZ	RAN	CIRC	SVRH	SIZE	HAIL	VIL	MAXZ	HT MXZ	BASE	TOP	DIR/SP
46	310	27	MESO	10%	<1.00	50%	33	61	14	2	28	228/45
1	304	66	WKCIRC	40%	1.00	70%	39	61	6	6	26	231/62
29	320	95		20%	<1.00	80%	19	50	21	11	30	228/64
67	332	71		0%	<1.00	0%	17	53	7	7	21	237/35
84	321	53		0%	<1.00	0%	16	53	5	5	25	220/49

CLOSE lft=LINKED CURSOR right=DRAW NEW LINE

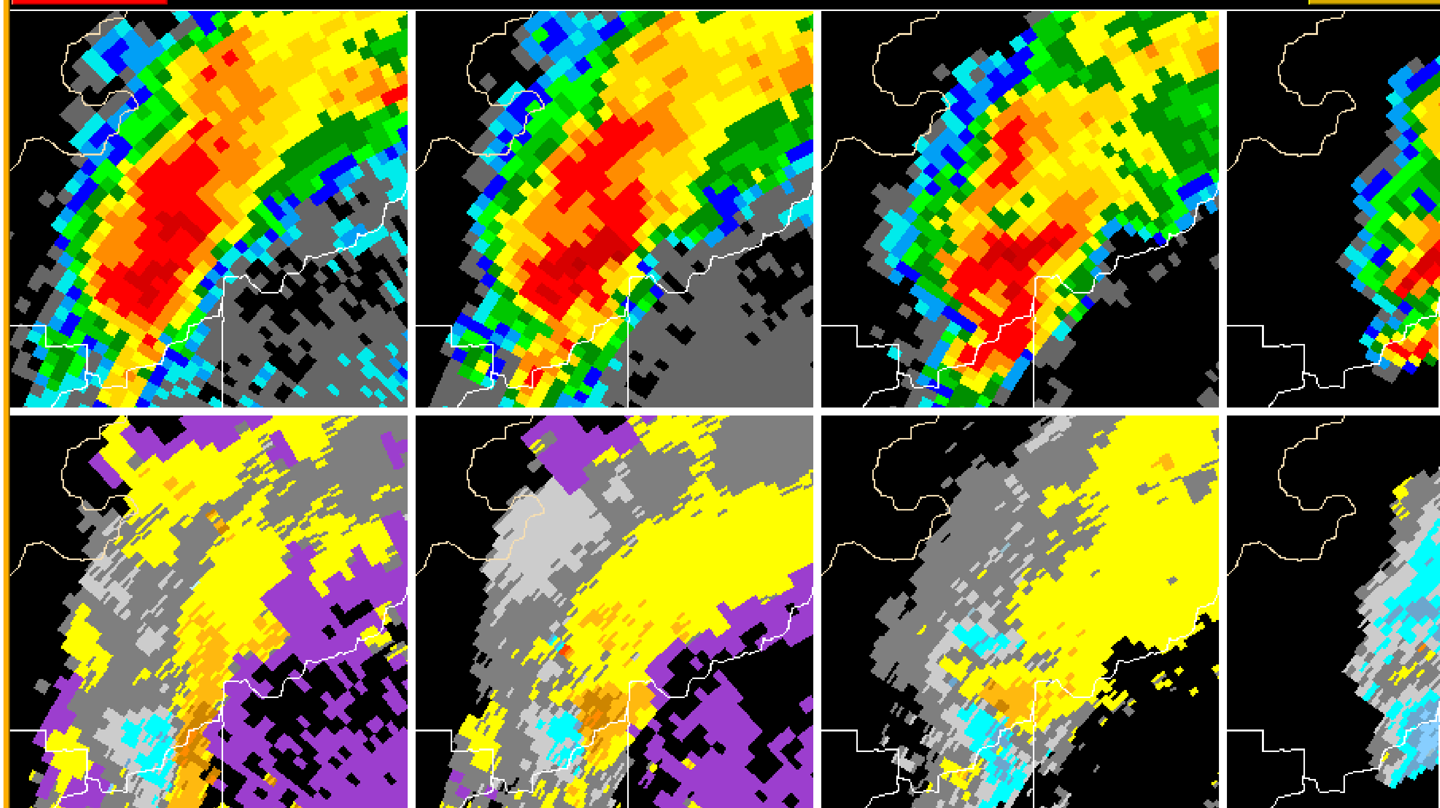

Win Prod Vol Swp (Az/Ran Ht)   Win Prod Vol Swp (Az/Ran Ht)   Win Prod Vol Swp (Az/Ran Ht)   Win Prod Vol S

1 DBZ 032 01 (315/027 1.8)   2 DBZ 032 02 (315/027 4.5)   3 DBZ 032 04 (315/027 9.9)   4 DBZ 032

5 SRV 032 01 (315/027 1.8)   6 SRV 032 02 (315/027 4.5)   7 SRV 032 04 (315/027 9.9)   8 SRV 032

Fig. 5. Same as Fig. 3, only 0031 UTC. The storm of interest has been reidentified as storm number 13 in the cell table.

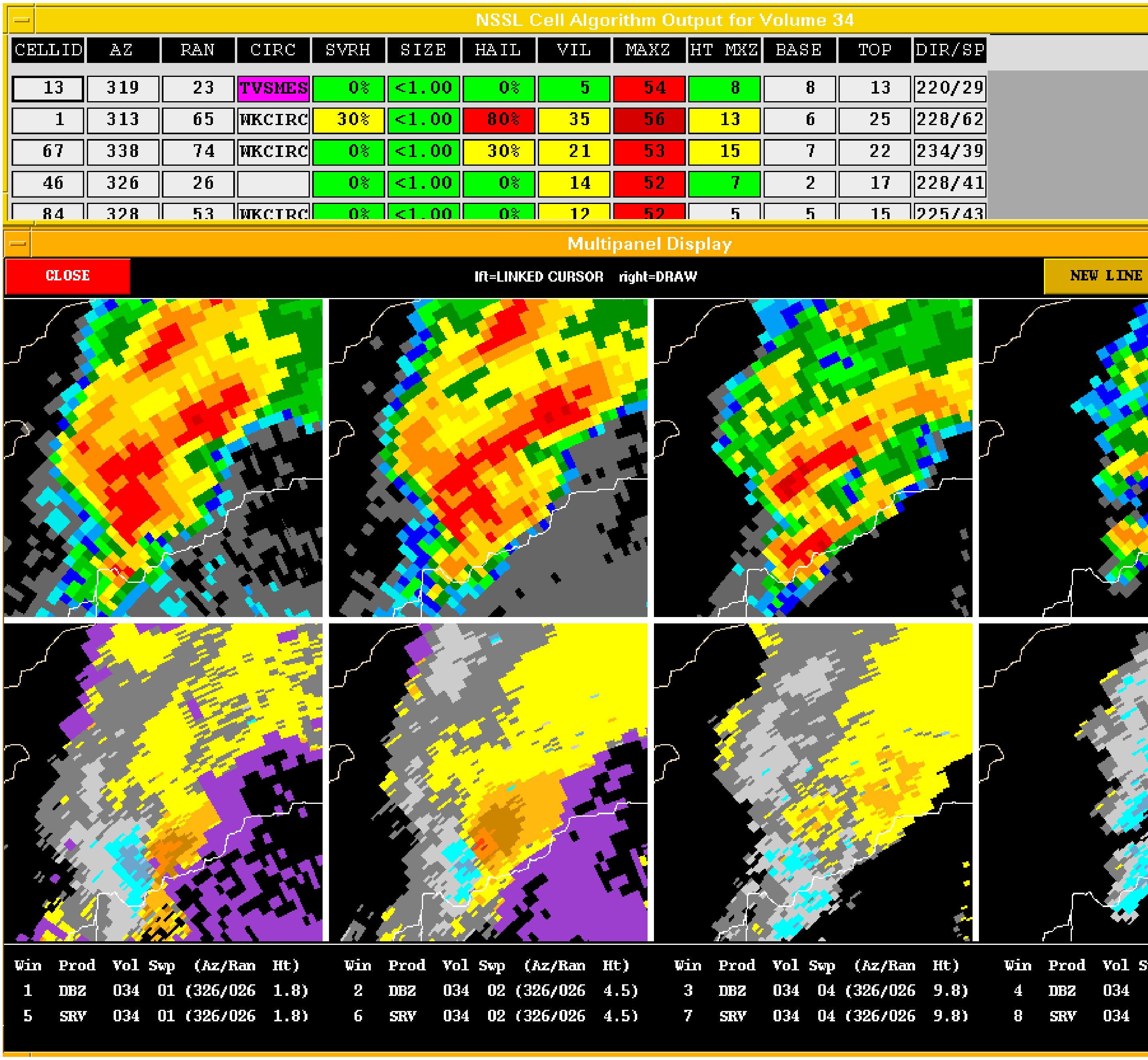

Fig. 6. Same as Fig. 3, only 0036 UTC.

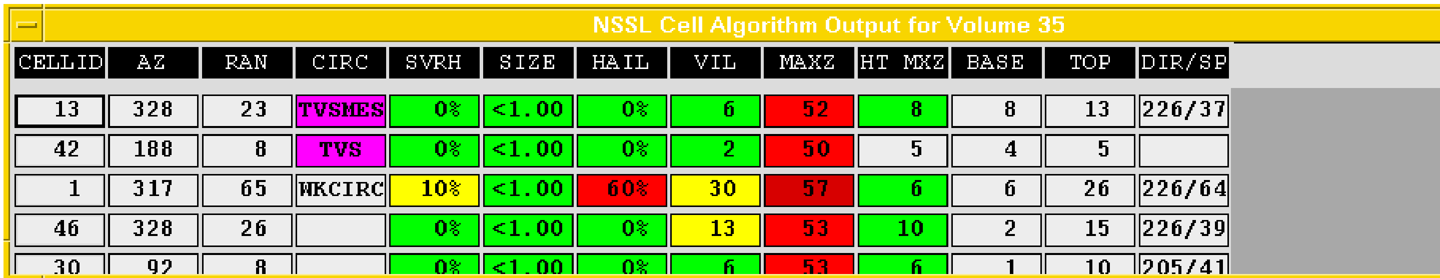

NSSL Cell Algorithm Output for Volume 35

CELLID	AZ	RAN	CIRC	SVRH	SIZE	HAIL	VIL	MAXZ	HT MXZ	BASE	TOP	DIR/SP
13	328	23	TVSMES	0%	<1.00	0%	6	52	8	8	13	226/37
42	188	8	TVS	0%	<1.00	0%	2	50	5	4	5	
1	317	65	WKCIRC	10%	<1.00	60%	30	57	6	6	26	226/64
46	328	26		0%	<1.00	0%	13	53	10	2	15	226/39
30	92	8		0%	<1.00	0%	6	53	6	1	10	205/41

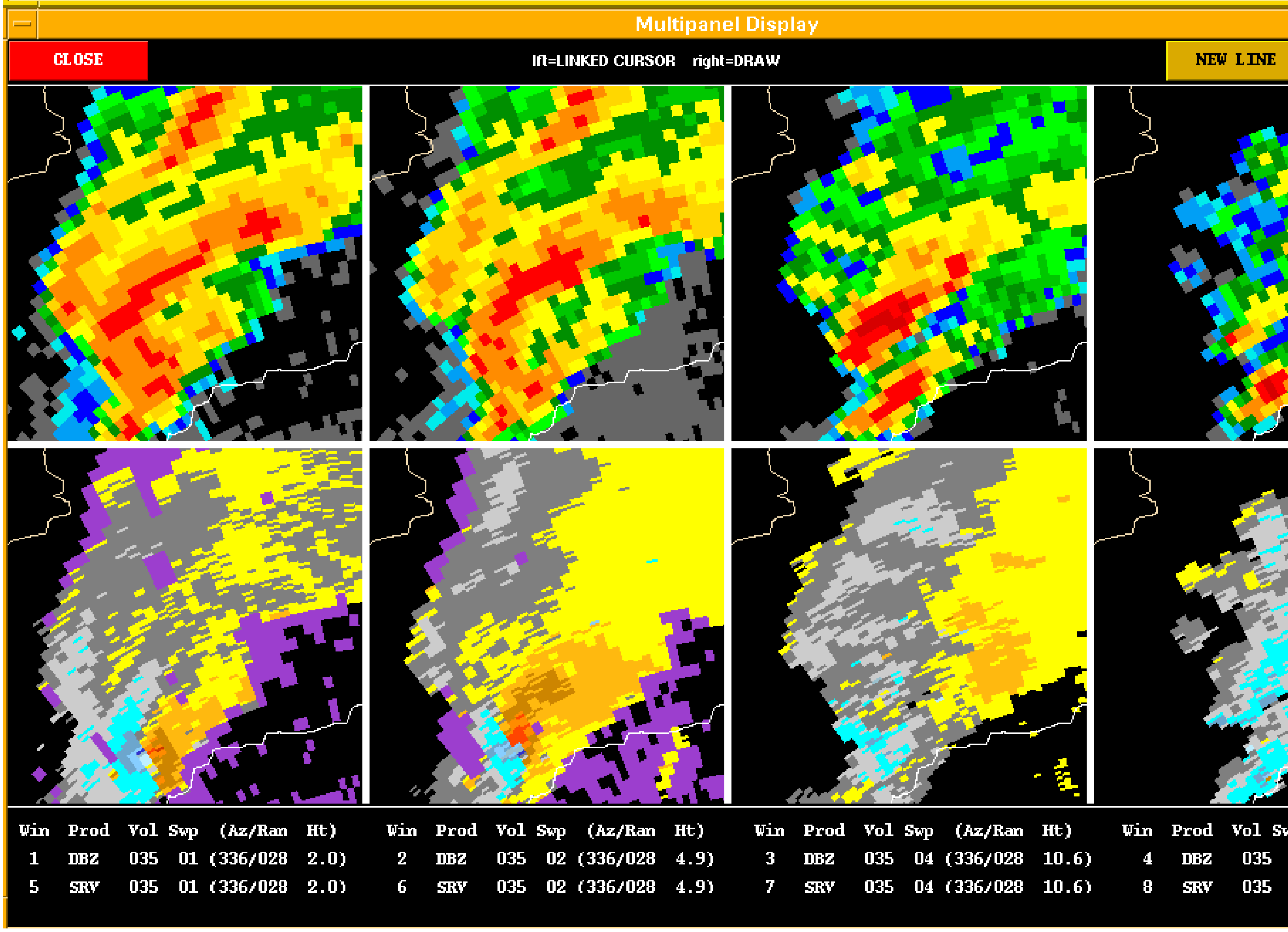

Fig. 7 . 6 panel radar display from the Jackson, MS, WSR-88D radar valid at 0051 UTC 10 December 1999. Top images are reflectivity, bottom images are storm relative velocity. From left to right, elevation angles are 0.5 degrees, 1.5 degrees, and 2.4 degrees.

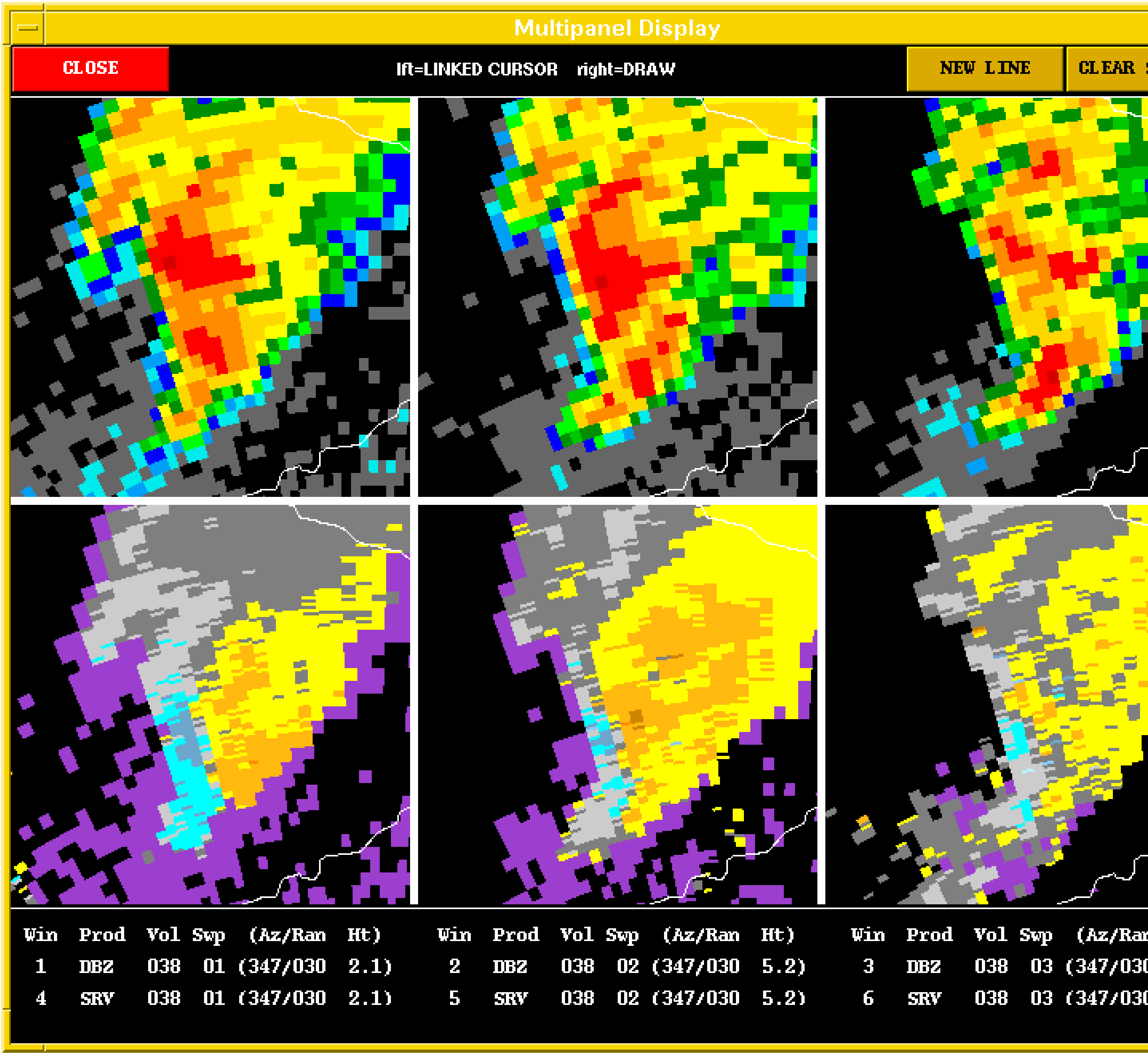

Fig. 8. Time height plot from WATADS at 0041 UTC of rotational velocity associated with Bentonia supercell.

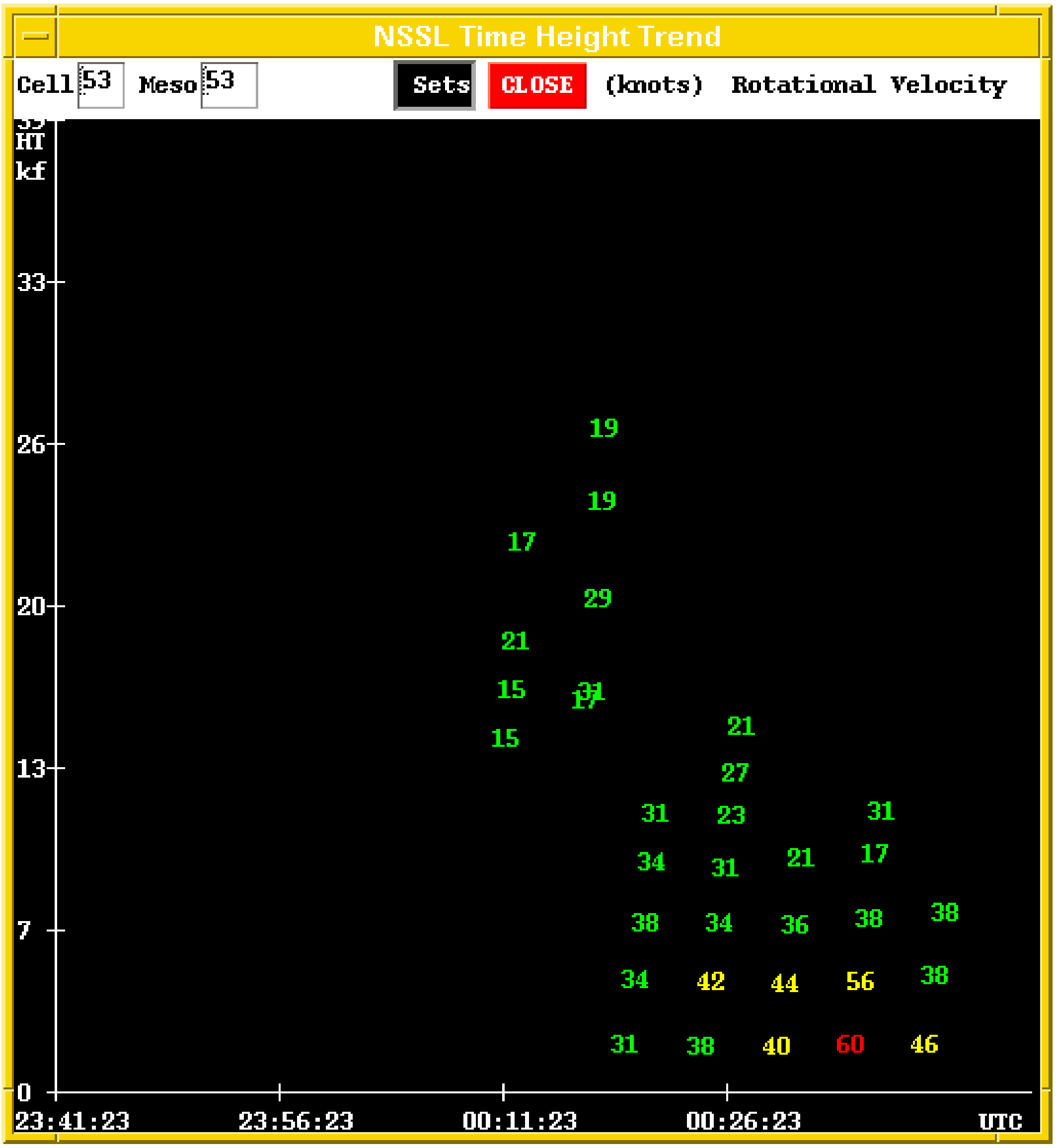

Fig. 9. Same as Fig. 7, only shear.

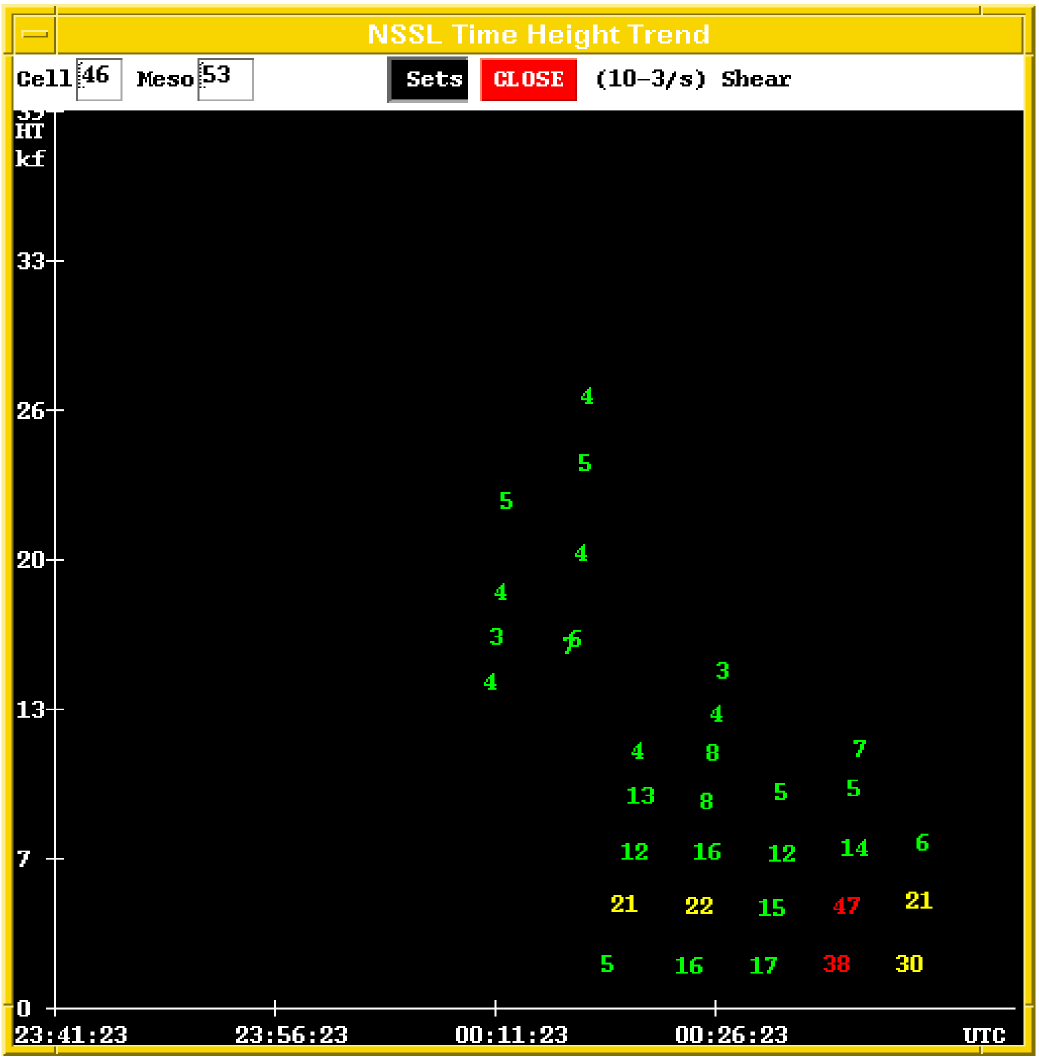

Fig. 10. Same as Figure 8, only for 0011 UTC.

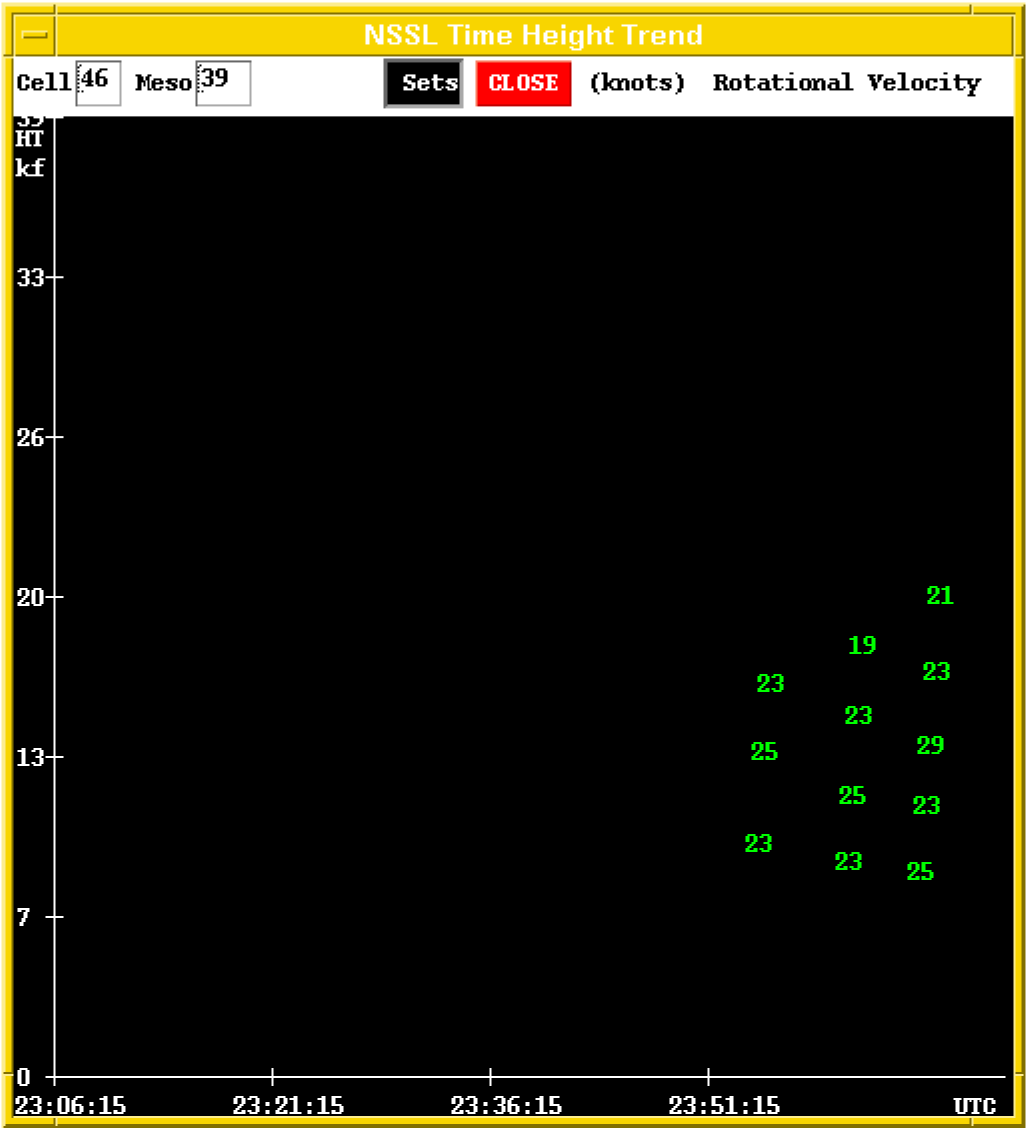

1. *Corresponding Author Address:* Alan E. Gerard, 234 Weather Service Dr., Jackson, MS, 39208; e-mail: Alan.E.Gerard@noaa.gov